



Characterization of Chlamydial Rho and the Role of Rho-Mediated Transcriptional Polarity during Interferon Gamma-Mediated Tryptophan Limitation

Scot P. Ouellette, a,b Parker R. Messerli, b Nicholas A. Wood, b Heather Hajovskyb

ABSTRACT As an obligate intracellular, developmentally regulated bacterium, Chlamydia is sensitive to amino acid fluctuations within its host cell. When human epithelial cells are treated with the cytokine interferon gamma (IFN-γ), the tryptophan (Trp)-degrading enzyme, indoleamine-2,3-dioxygenase, is induced. Chlamydiae within such cells are starved for Trp and enter a state of so-called persistence. Chlamydia lacks the stringent response used by many eubacteria to respond to this stress. Unusually, chlamydial transcription is globally elevated during Trp starvation with transcripts for Trp codon-containing genes disproportionately increased. Yet, the presence of Trp codons destabilized 3' ends of transcripts in operons or large genes. We initially hypothesized that ribosome stalling on Trp codons rendered the 3' ends sensitive to RNase activity. The half-life of chlamydial transcripts containing different numbers of Trp codons was thus measured in untreated and IFN-γ-treated infected cells to determine whether Trp codons influenced the stability of transcripts. However, no effect of Trp codon content was detected. Therefore, we investigated whether Rho-dependent transcription termination could play a role in mediating transcript instability. Rho is expressed as a midcycle gene product, interacts with itself as predicted, and is present in all chlamydial species. Inhibition of Rho via the Rho-specific antibiotic, bicyclomycin, and overexpression of Rho are detrimental to chlamydiae. Finally, when we measured transcript abundance 3' to Trp codons in the presence of bicyclomycin, we observed that transcript abundance increased. These data are the first to demonstrate the importance of Rho in Chlamydia and the role of Rho-dependent transcription polarity during persistence.

KEYWORDS *Chlamydia*, stringent response, interferon gamma, transcription termination, persistence, Rho

chlamydia is a developmentally regulated, obligate intracellular bacterium. These unique bacteria alternate between functionally and morphologically distinct forms during their developmental cycle (see reference 1 for a review). The elementary body, or EB, mediates attachment and internalization into a susceptible host cell, whereas the reticulate body, or RB, grows and divides within a membrane-bound pathogen-specified parasitic organelle termed an inclusion (2). At the end of the developmental cycle, RBs differentiate back to EBs and are released from the cell to initiate a new round of infection. In evolving to obligate intracellular growth, chlamydiae have undergone significant reductive evolution. These pathogens have streamlined their genomes by eliminating superfluous pathways and genes (3). Conversely, if they have maintained a set of genes, then it is likely important for the bacteria.

Chlamydiae are pathogens that cause a range of illnesses in humans and animals

Received 29 March 2018 Returned for modification 24 April 2018 Accepted 27 April 2018

Accepted manuscript posted online 30 April 2018

Citation Ouellette SP, Messerli PR, Wood NA, Hajovsky H. 2018. Characterization of chlamydial Rho and the role of Rho-mediated transcriptional polarity during interferon gamma-mediated tryptophan limitation. Infect Immun 86:e00240-18. https://doi.org/10.1128/

Editor Craig R. Roy, Yale University School of Medicine

Copyright © 2018 American Society for Microbiology. All Rights Reserved.

Address correspondence to Scot P. Ouellette, scot.ouellette@unmc.edu.

^aDepartment of Pathology and Microbiology, College of Medicine, University of Nebraska Medical Center, Omaha, Nebraska, USA

^bDivision of Basic Biomedical Sciences, Sanford School of Medicine, University of South Dakota, Vermillion, South Dakota, USA

(4-7). Within humans, Chlamydia trachomatis and Chlamydia pneumoniae are the primary agents of chlamydial diseases. Of clinical significance is that chlamydial infections are often unrecognized and asymptomatic, which can lead to chronic sequelae. These can include pelvic inflammatory disease, tubal factor infertility, and reactive arthritis for C. trachomatis (8, 9) and possibly atherosclerosis and adult-onset asthma, among other illnesses, for C. pneumoniae (10, 11). One hypothesis for asymptomatic chlamydial infections is that the organisms enter a nonproductive growth state referred to as persistence.

Chlamydial persistence is defined as a state of culture-negative but viable growth wherein cell division is blocked and the bacteria are morphologically aberrant (12, 13). In vitro, persistence is induced primarily by nutrient limitation (14-19). As chlamydiae depend on their host cell for most of their nutritional needs, when the host cell is starved, so are the bacteria. Interferon gamma (IFN- γ) treatment of human epithelial cells induces expression of the enzyme indoleamine-2,3-dioxygenase (IDO), which cleaves tryptophan (Trp or W) to produce N-formyl-kynurenine (20-23). C. trachomatis and C. pneumoniae are Trp auxotrophs and acquire this essential amino acid from the host cell via free amino acids in the cytosol or uptake of lysosomal degradation products (24). Some C. trachomatis serovars can convert indole, presumably supplied by the microbiota, to Trp (25, 26). Once starved of Trp, the chlamydial developmental cycle is diverted to persistence. However, reactivation of productive growth with continued progress through the developmental cycle can be restored by removal of IFN- γ (27). In cell culture, IFN-y-mediated Trp limitation is a model system for inducing a reproducible amino acid stress response in Chlamydia.

We previously investigated chlamydial transcription during IFN-γ-mediated persistence and found that transcription was globally increased whereas translation was globally decreased (28). Importantly, transcriptional responses of orthologous genes during IFN-γ-mediated persistence between C. trachomatis and C. pneumoniae are also similar (e.g., euo and omcB [28]). More recently, we hypothesized, and presented evidence in C. pneumoniae, that the Trp codon content of a gene influences its transcription during Trp limitation (29). Interestingly, we found that the transcription of genes with multiple Trp codons was significantly increased whereas for those genes lacking Trp codons, no change in transcription was detected. However, we did observe that, within operons or large genes, the presence of Trp codons had a destabilizing effect on the 3' end of the transcript. These findings are consistent with a model in which ribosome stalling on Trp codons destabilizes downstream messages.

The current work was designed to understand why Trp codons cause the 3' ends of their respective transcripts to become less abundant during Trp starvation. We hypothesized that one of two effects could be occurring. Under Trp-replete conditions, ribosomes translate efficiently across Trp codons and protect the message from degradation. When Trp is limiting or absent, ribosomes will stall at Trp codons. We hypothesized that this would lead to the transcript 3' to the stalled ribosomes either becoming susceptible to ribonucleases (RNases) or becoming available for Rho binding through internal Rho sites to terminate transcription prematurely, termed Rho-dependent polarity. These possibilities are depicted in Fig. 1. In the former case, this would lead to an increase in the stability of Trp codon-rich transcripts protected by ribosomes. In the latter case, Rho, a well-described transcriptional terminator in prokaryotes, would bind RNA and translocate along it until it catches the RNA polymerase (RNAP), where it induces disassociation of the RNAP from the DNA template (30). However, in testing the first possibility, we observed no effect of Trp codons on transcript stability. Therefore, we initiated a series of studies to test the function of Rho in mediating transcript termination via Rho-dependent polarity during Trp starvation and to determine the importance of Rho more generally in Chlamydia. Our data are consistent with a model wherein the presence of Trp codons in transcripts induces ribosome arrest that leads to Rho-dependent polarity and transcription termination. These data are the first to demonstrate the importance of Rho in Chlamydia and its critical role in chlamydial persistence.

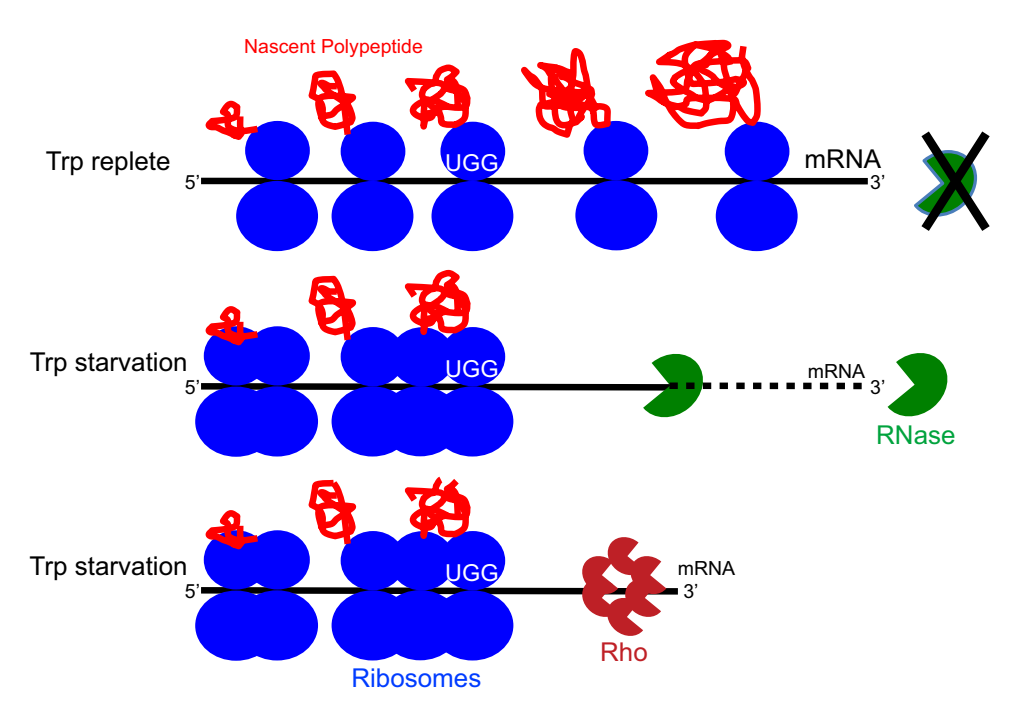


FIG 1 Model for transcript instability during IFN-γ-mediated Trp starvation. Hypothetical model for transcript stability before and after tryptophan (Trp) codons under normal and Trp starvation conditions. Under normal culture conditions (Trp replete), ribosomes translate the entire mRNA, thus blocking any aberrant RNase activity. During Trp starvation, the ribosomes are blocked from or impaired in progressing beyond the Trp codon (UGG). In these circumstances, one of two possibilities is proposed to explain the decrease in transcript abundance: (i) the 3' end of mRNA becomes accessible to RNase degradation, or (ii) Rho-dependent polarity effects occur when Rho binds exposed sites on the transcript. This could occur in either monocistronic or polycistronic messages with Trp codons.

RESULTS

Measurement of transcript stability as a function of Trp codon content. We previously observed that chlamydial Trp codon-containing transcripts were disproportionately increased during IFN- γ -mediated Trp starvation (29). We hypothesized that ribosome stalling on Trp codons near the 5' end of the transcript would render the 3' end susceptible to RNase degradation while simultaneously stabilizing the 5' end. Conversely, we anticipated that the stability of transcripts lacking Trp codons would be unaffected by Trp starvation. To test this hypothesis, we extracted nucleic acids from *C. pneumoniae*-infected cultures, treated or not with IFN- γ , in the presence or absence of rifampin to block RNA polymerase activity. Transcript abundance was measured by reverse transcriptase quantitative PCR (RT-qPCR), and the half-life of each transcript was calculated.

We assessed 11 transcripts from genes carrying 0 to 11 Trp codons and involved in metal import, cell division, transcription, and a variety of other cellular processes. Two different sets of genes, ytgA-ytgD and $rnhB_1-metG$, were parts of polycistronic operons with high and low Trp codon density in the 5' gene, respectively (29). This allowed us to test the effects of Trp codons on transcript stability within a single transcript. All these target genes had been previously assessed by us for their transcriptional pattern during IFN- γ -mediated Trp limitation and, importantly, have orthologs in *C. trachomatis* (29). All primer sets were designed to bind within the first third of the nucleotide sequence of the gene and, when possible, 5' to all Trp codons (29). For untreated cultures, half-life measurements were made at 24 hours postinfection (hpi), when *C. pneumoniae* RBs are actively transcribing, except for the late gene omcB, in which case the half-life was calculated at 48 hpi, when it is actively transcribed. For IFN- γ -treated cultures, half-life measurements were made at 48 hpi, when the transcriptional effects of IFN- γ are detectable (29).

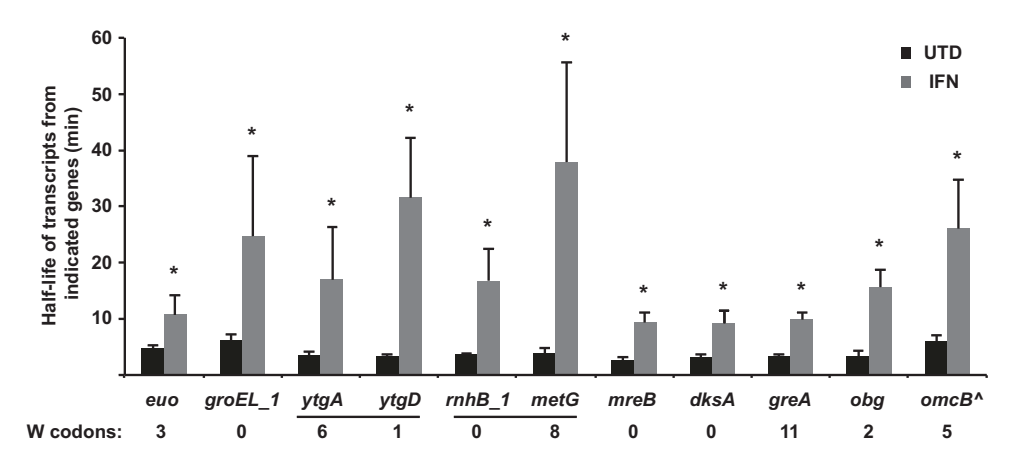


FIG 2 Measure of transcript stability as a function of Trp codon content. The human epithelial cell line HEp2 was infected with C. pneumoniae AR39 and treated with interferon gamma (IFN) or not treated (UTD) at the time of infection. At 24 hpi, transcription was blocked in UTD cultures by the addition of rifampin, whereas rifampin was added at 48 hpi for IFN-y-treated cultures. Nucleic acid samples were collected at these time points and 15 min after rifampin addition. Transcript levels were quantified by RT-qPCR and normalized to genomic DNA levels, and the half-life of transcripts for each gene, on the x axis, was calculated in minutes, on the y axis. The number of tryptophan (W) codons present in the genes is indicated. The bars under ytgA and ytgD and, separately, under rnhB_1 and metG indicate that these genes are present in the same operon. For omcB, a late gene, the half-life of the message in UTD cultures was calculated at 48 hpi, when it is actively transcribed ($^{\wedge}$). *, P < 0.05 by one-tailed Student's t test.

As observed in Fig. 2, the average half-life of chlamydial transcripts measured after 15 min of rifampin addition was generally increased during IFN-γ-mediated Trp starvation (3.92 min in untreated [UTD] versus 18.95 min in IFN-γ-treated samples). However, there was no correlation between transcript half-life and the presence of Trp codons within the transcript. This was also true when the half-life was measured after 30 min of rifampin treatment (see Fig. S1 in the supplemental material). The 3' ends of the transcripts for the ytq and rnhB_1 operons appeared more stable than the 5' end. Consequently, our hypothesis was disproved and rejected. Recently, a study analyzing transcript stability in Chlamydia by transcriptome sequencing (RNA-seq) was published, in which half-lives were measured to be approximately 15 min (31). However, our results are consistent with other measures of bacterial transcript stability (see reference 32 for a review). In addition, our methodology (using RT-qPCR) requires less handling/ modification of the RNA samples than does RNA-seq and is likely more reliable because of this.

Chlamydia encodes a Rho homolog with an extended N terminus. As our first hypothesis was invalidated, we next hypothesized that transcript instability may be due to Rho-dependent polarity (33–36). Rho is a transcription terminator that acts as a hexameric helicase (33). In this scenario, ribosome stalling at Trp codons would render rut (Rho utilization) sites accessible to Rho, leading to premature transcript termination. Rho contains a conserved N-terminal domain, an RNA-binding domain, and an ATPase domain containing Walker A and B motifs, which allows it to translocate along mRNA transcripts. A basic schematic of Rho is illustrated in Fig. 3A. Rho is essential in most bacteria in which it has been studied (37), and all Chlamydia species encode a Rho homolog (from our analysis of publicly available genome sequences). Interestingly, chlamydial Rho contains an additional N-terminal region (amino acids 1 to 49) in almost all strains and species of Chlamydia that is absent in Escherichia coli and most Gramnegative Rho homologs but present in other types of bacteria, including Mycobacterium tuberculosis. Given that Chlamydia has undergone extensive genomic reduction in evolving to obligate intracellular dependence, the fact that this sequence has not been deleted indicates a potentially important function for the organism. In the very few chlamydial strains lacking these additional residues, there is a methionine residue in place of a valine (V46 in sequence), and thus it is likely that the start site has been

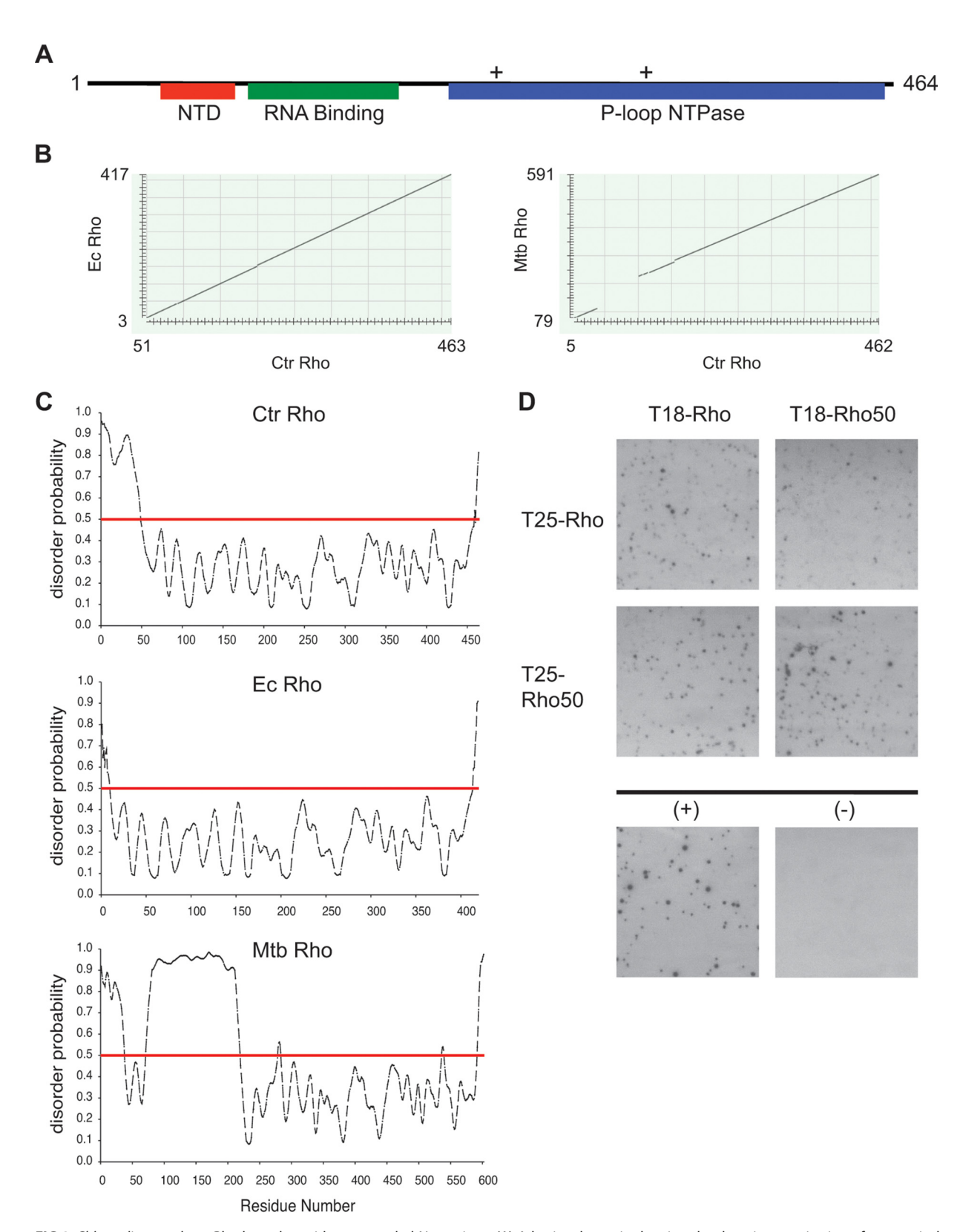


FIG 3 Chlamydia encodes a Rho homolog with an extended N terminus. (A) A basic schematic showing the domain organization of a canonical Rho protein with a conserved N-terminal domain (NTD), an RNA binding domain, and a P-loop NTPase domain with Walker motifs indicated by a plus sign (+). (B) BLAST alignment of C. trachomatis (Ctr) Rho versus E. coli (Ec) Rho and M. tuberculosis (Mtb) Rho with associated amino acids aligned indicated by the numbers on the axes. (C) Protein disorder prediction plots for the Rho homologs depicted in panel B. The red line indicates the threshold value for a false-positive rate of 5% with the overall predicted disorder probability indicated on the y axis and the associated amino acids from the N terminus to the C terminus increasing along the x axis. (D) Bacterial two-hybrid (BACTH) test of the ability of chlamydial Rho to interact with itself. Full-length Rho or a truncated mutant lacking the first 49 amino acids, Rho50, was fused to each of the T25

misannotated. A recent article described a role for an extended N-terminal domain of Rho from *Clostridium botulinum* in prion formation (38). However, the extended chlamydial domain does not align to any identified sequences aside from *Chlamydia* species, based on our analysis of publicly available genome sequences. We hypothesize that this domain may be important for mediating interactions with either itself or other factors (e.g., protein or metabolite).

To begin an investigation into Rho function in *Chlamydia*, we initiated basic bioinformatics analyses. *C. pneumoniae* and *C. trachomatis* Rho proteins are 88% identical and 92% similar, with both proteins containing 464 amino acids. *C. trachomatis* Rho is also highly homologous to both *E. coli* (61% identical, 78% similar over 99% of *E. coli* Rho with an E value of 0) and *M. tuberculosis* (53% identical, 72% similar over 67% of *M. tuberculosis* Rho with an E value of 8e–146) and aligns well with both of these homologs (Fig. 3B). The variability within Rho between the chlamydial species is localized to the extended N terminus, and if these amino acids are excluded from alignments, then *C. pneumoniae* and *C. trachomatis* Rho are even more highly conserved (94% identical and 96% similar). This additional domain is predicted to be disordered within the Rho protein, similar to *M. tuberculosis* Rho (Fig. 3C), suggesting potential additional functionality to chlamydial Rho or additional determinants that govern the proper folding or interactions of this domain.

To test whether chlamydial Rho is capable of interacting with itself and whether the additional N-terminal residues are important for homotypic interactions, we employed the bacterial adenylate cyclase-based two-hybrid (BACTH) system to monitor protein-protein interactions. This system is predicated on the ability of two complementary fragments of the adenylate cyclase toxin, T25 and T18, of *B. pertussis* to reconstitute enzyme activity when brought into close proximity by interacting proteins (39). When an adenylate cyclase mutant of *E. coli* was cotransformed with plasmids expressing T25-and T18-Rho, a positive interaction was detected (Fig. 3D), indicating the ability of chlamydial Rho to interact with itself. This was also true for plasmids expressing the truncated mutant of Rho, Rho50. The truncated mutant also retained the ability to interact with full-length Rho. Thus, we conclude that the additional N-terminal 49 amino acids of chlamydial Rho do not function in the ability of this protein to interact with itself and likely have an alternative role *in vivo*, which requires further study.

Chlamydial Rho is expressed as an RB product. We next sought to determine the expression pattern of chlamydial Rho. As chlamydiae are developmentally regulated bacteria, they transition between functional and morphological forms (EBs and RBs), and chlamydial gene expression can be broadly divided into three classes that coincide with differentiation from EB to RB (early), RB growth and division (midcycle), and differentiation from RB to EB (late) (40). We previously noted that C. pneumoniae rho transcription peaks at 24 hpi, coinciding with the midcycle phase in this species, and is unchanged during IFN-γ-mediated Trp starvation as it carries no Trp codons (29). To confirm and more accurately assess rho transcription over a developmental cycle, we assessed the transcriptional profiles of C. trachomatis rho and control genes representing the different classes by RT-qPCR to determine which of these classes best described its expression profile. Total RNA and DNA were collected over a time course of infection with C. trachomatis L2. As seen in Fig. 4, the transcriptional pattern of rho most closely resembles that of ftsl, a midcycle cell division-associated gene, as opposed to ct135, an early gene, or IcrH_1, a late gene. This is consistent with C. pneumoniae rho transcription, which also peaks during the midcycle RB phase of the developmental cycle (29).

Determination of the effect of overexpression of Rho on chlamydial growth. It is currently not possible to transform *C. pneumoniae*. However, with the recent ability

FIG 3 Legend (Continued)

or T18 fragments of the adenylate cyclase domain of *B. pertussis*. Plasmids encoding these constructs were cotransformed into *E. coli* DHT1 cells and plated on minimal medium. Interacting proteins reconstitute adenylate cyclase activity, which results in blue colonies when grown on X-Gal. A positive (+) control of T25-zip and T18-zip, encoding the GCN4 leucine zipper motifs, is shown, as is a negative (-) control of T25-Rho and T18 only (i.e., empty vector).

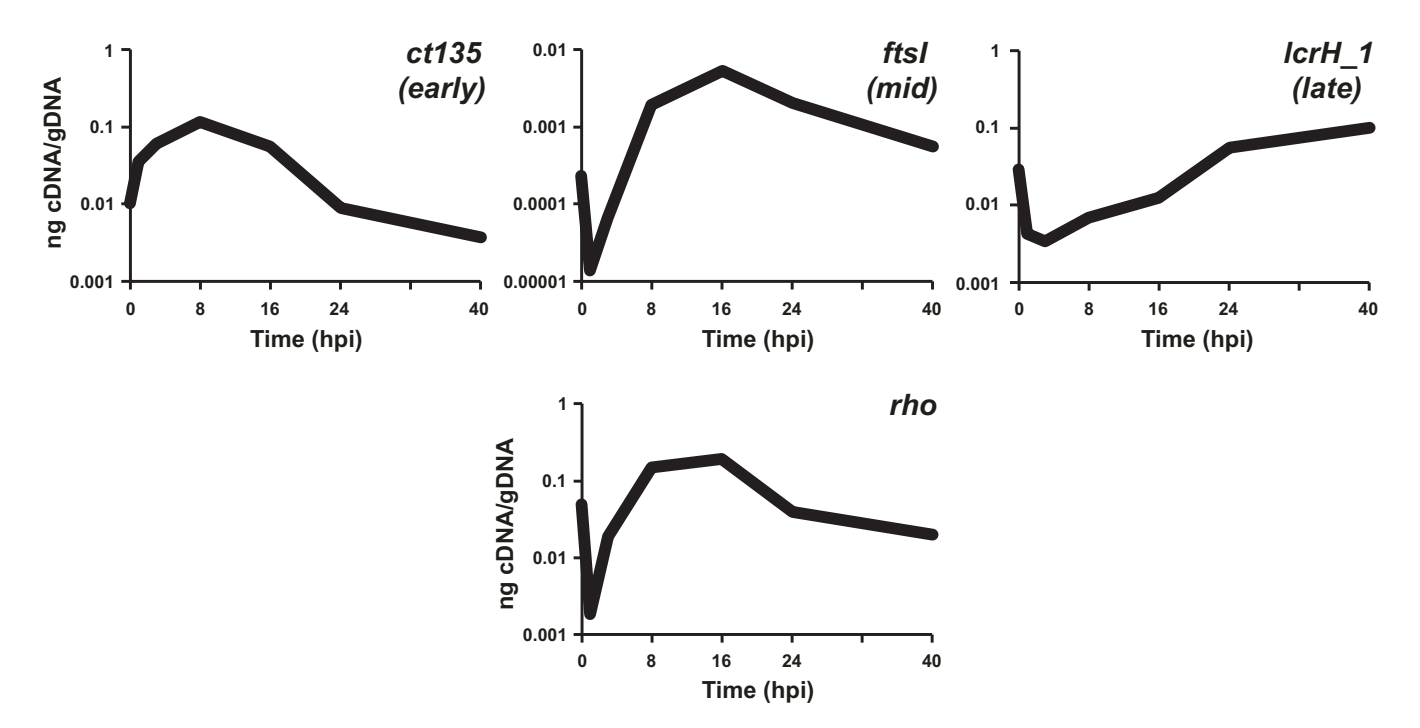


FIG 4 Chlamydial Rho is expressed as an RB product. Nucleic acid samples were collected over a time course from *C. trachomatis* L2-infected HEp-2 cells. Transcripts (cDNA) were quantified by RT-qPCR and normalized to genomic DNA (gDNA) using a standard curve. The indicated genes represent the different developmental stages, including early (*ct135*), midcycle (*ftsI*), and late (*lcrH*_1). Note that *rho* is transcribed similarly to *ftsI*. These data are the averages from at least two experiments analyzed in triplicate with standard deviations typically less than 10% of the averages.

to transform Chlamydia trachomatis with a shuttle vector having been developed by the Clarke lab (41), we sought to take advantage of this, along with an inducible expression system developed by the Hefty lab (42), to determine what effect overexpression of Rho would have on chlamydial growth. Reports in the literature indicate that overexpression of nonessential proteins, such as green fluorescent protein (GFP) or IncA, in C. trachomatis have no biologically significant effect on chlamydial growth whereas overexpression of essential proteins, such as the cell division protein FtsQ, leads to aberrant bacterial morphologies and stalled growth (43, 44). We constructed a shuttle vector encoding an anhydrotetracycline (aTc)-inducible 6×His-tagged chlamydial Rho (Rho-6xH) and used this to transform C. trachomatis L2. When cells were infected and aTc was added at 10 hpi, we observed a strong $6\times$ His signal in the bacterial cytosol after 6 h of induction consistent with the predicted localization of Rho. The morphology of the bacteria was normal with typical RB forms visualized around the periphery of the inclusion membrane (Fig. 5). However, after 12 h of induction (a total of 22 h of infection), we failed to observe any further development of the chlamydial forms whereas the untreated cultures continued to develop normally. Rather, we detected inclusions that appeared no different in size or bacterial numbers from those observed after 6 h of induction. A similar effect was observed for the truncation mutant Rho50-6xH, lacking the first 49 amino acids of Rho (data not shown), thus indicating that this effect is not attributable to these additional amino acids. We routinely observed aberrantly enlarged bacteria typical of persistent chlamydiae that are blocked in cell division in the organisms expressing most strongly the Rho-6xH protein. This did not appear to be an effect of simply overexpressing an exogenous protein, as a C. trachomatis transformant expressing a predicted nonfunctional Rho-6xH with a mutation (D311A) in the Walker B motif failed to display this phenotype (see Fig. S2 in the supplemental material). This observation suggests that the expression of the Walker B mutant, presumably impaired in its ATPase activity, could not sufficiently interfere with the normal function of endogenous Rho. However, we cannot exclude the possibility that the mutant protein, while clearly expressed with the 6×His at the C terminus, does

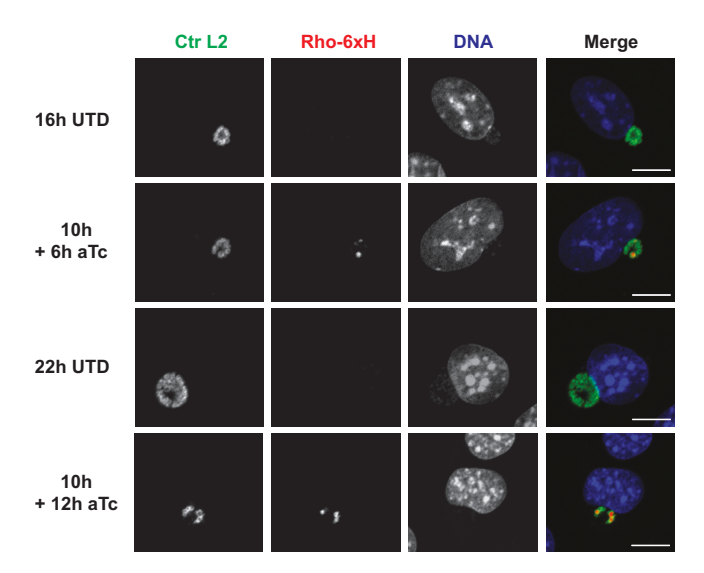


FIG 5 Determination of the effects of overexpression of Rho on chlamydial growth. *C. trachomatis* L2 (Ctr L2) was transformed with an anhydrotetracycline (aTc)-inducible vector encoding $6 \times \text{His}$ -tagged Rho (Rho-6xH). McCoy cells were infected with the transformant and cultured in the presence of 1 U ml $^{-1}$ penicillin. At 10 hpi, expression of Rho-6xH was induced in a subset of wells by adding aTc. At 16 hpi and 22 hpi, cells were fixed in methanol and processed for immunofluorescence microscopy with images acquired at a magnification of $\times 40$ with a $4 \times$ digital zoom on a Zeiss LSM710 confocal microscope. Bars, 10 μ m.

not fold properly to interact with native Rho in *Chlamydia*. Interestingly, we have been unable to plaque purify the Rho-6xH or Rho50-6xH transformants, as we routinely observe mixed morphologies of inclusions, suggesting that some leakiness of expression is not well tolerated, possibly leading to plasmid instability. This, unfortunately, precludes population-wide transcriptional analyses of the effects of overexpression of the $6\times$ His-tagged constructs since there is a mixed population. Taking both the long-term induction effects and the inability to isolate clonal populations of transformants, we interpret this as a deleterious effect of extended Rho expression on chlamydial growth, which supports the likelihood that Rho is essential to *Chlamydia*.

Chlamydia is inhibited by the Rho-specific antibiotic, bicyclomycin. We anticipated that Rho would be an essential protein in Chlamydia and thus not a potential target for gene disruption by recently developed techniques (45, 46). However, a Rho-specific antibiotic exists, called bicyclomycin (Bic) (47), which allowed us to probe the essentiality of Rho in Chlamydia via a chemical genetic approach. Bicyclomycin is a reversible, noncompetitive inhibitor of Rho that interferes with its ATPase activity and ability to translocate along mRNA (48). When we treated C. pneumoniae-infected cultures with bicyclomycin, we did not observe any recoverable infectious organisms (data not shown). To determine if Bic could block C. trachomatis growth, we treated C. trachomatis L2-infected cultures with various doses of Bic and quantified the infectious EB yield through an inclusion-forming unit (IFU) assay. C. trachomatis L2 is the fastestgrowing human-infecting species (49), and we observed that its growth was sensitive to Bic with little to no detectable growth with treatments as low as 5 μ g ml⁻¹ added at the time of infection (Fig. 6A). Furthermore, C. trachomatis L2 growth was inhibited effectively by treatment as late as 12 hpi (beginning of log-phase RB growth [Fig. 6B]) or during the first 12 h of infection only (EB-to-RB differentiation and lag phase; data not shown). Conversely, pretreatment of EBs or treatment during only the first hour of infection (to test effects on attachment and entry) had no biologically significant impact on growth (data not shown). To date, we have been unable to isolate a bicyclomycinresistant mutant of C. trachomatis, and we believe this to be due to the instability of the drug over extended treatment times resulting in heterotypic resistance.

We next wanted to determine whether the inhibition by Bic of *Chlamydia* was a static or cidal effect. We therefore treated infected cultures with two different inhibitory

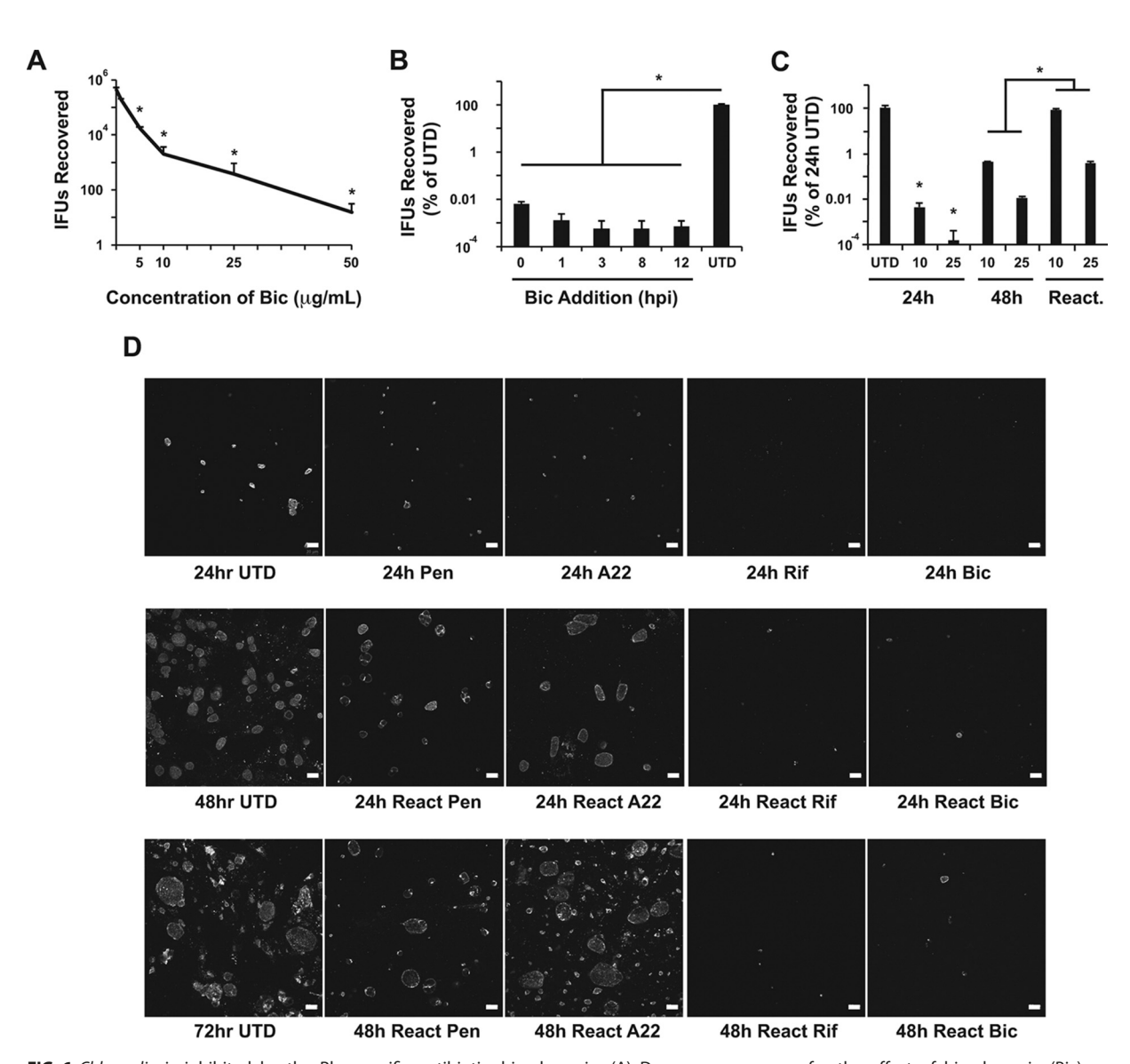


FIG 6 Chlamydia is inhibited by the Rho-specific antibiotic, bicyclomycin. (A) Dose-response curve for the effect of bicyclomycin (Bic) on chlamydial growth. HEp-2 human epithelial cells were infected with C. trachomatis L2 and treated at the time of infection with the indicated concentration of Bic. After 24 h of infection, cells were lysed and used to reinfect a fresh HEp-2 cell layer to quantify the inclusion-forming units (IFUs). (B) Determination of the effects of Bic when added at different time points during infection. HEp-2 cells were infected as described above and treated with 25 µg ml⁻¹ Bic at the indicated times, in hours postinfection (hpi). IFUs were quantified as described above. (C) Test of cidal activity of Bic on Chlamydia. HEp-2 cells were infected and treated or not (UTD) at the time of infection with the indicated concentrations (in micrograms per milliliter) of Bic. In a subset of wells, the antibiotic was washed out at 24 hpi and replaced with fresh medium (React.) to determine if the drug was static or cidal. IFUs were quantified at 24 and 48 hpi (React. at 48 hpi). Data in panels B and C were normalized to the IFUs recovered from the 24-hpi untreated wells. Data for all figures are representative of at least two experiments with the averages and standard deviations shown. For panels A to C, an asterisk (*) indicates a P value of <0.05 by one-tailed Student's t test. For panels A and B, the significance is in comparison to the UTD sample. For panel C, the significance is in comparison to UTD samples at the 24-h time point, but for the reactivated (React.) samples significance is in comparison to the 48-h time point for the respective Bic-treated samples. (D) Immunofluorescence analysis of the effects of known static and cidal antibiotics on chlamydial growth compared to the effects observed with Bic. HEp2 cells were infected with C. trachomatis L2 and treated with the indicated antibiotics. The static antibiotics penicillin (Pen) and A22, targeting chlamydial cell division, and the cidal antibiotic rifampin (Rif) were used. At 24 hpi, one set of samples was fixed, whereas the others were washed three times with the subsequent addition of fresh medium without antibiotics to reactivate (React) chlamydial growth at 24 h and 48 h postreactivation (total, 48 h and 72 h). Bars, 20 μ m.

doses, $10~\mu g~ml^{-1}$ and $25~\mu g~ml^{-1}$, of Bic for 24 h following infection and then washed out the antibiotic and further cultured for another 24 h before quantifying IFU output. As seen in Fig. 6C, the two doses of Bic were able to significantly inhibit chlamydial growth as late as 48 h in culture, although IFUs increased for both doses at 48 h compared to 24 h. This suggests either that the drug is losing stability in culture or that

the bacteria are beginning to outgrow its effects (e.g., heterotypic resistance). Once the drug was removed at 24 hpi, more-robust chlamydial growth was seen in the culture originally treated with the lower ($10-\mu g\ ml^{-1}$) concentration, whereas the culture initially treated with the higher ($25-\mu g\ ml^{-1}$) concentration still resulted in a >2-log inhibition compared to the 24-h untreated sample.

We compared the ability of Bic to effectively block chlamydial growth to those of known antibiotic inhibitors of Chlamydia that are static or cidal. Penicillin (Pen) and A22 target chlamydial cell division (50) and are static to chlamydiae, resulting in reactivation of productive growth after removal of the antibiotic from the culture medium. Rifampin (Rif) is considered cidal to chlamydiae with little to no recovery of productive growth after removal from the medium (51). C. trachomatis L2-infected cells were treated with each of these antibiotics and Bic and, at 24 h postinfection, the drugs were removed from the medium with three washes before adding fresh medium without antibiotics. The recovery of chlamydial growth was monitored by immunofluorescence analysis of inclusion growth and development for a further 48 h to assess the ability of chlamydiae to recover from the antibiotic treatment (Fig. 6D). As expected, removal of Pen or A22 from the medium resulted in the outgrowth of chlamydiae as indicated by the detection of large inclusions. For Pen, a mixture of normal and sensitive bacteria was still detected 24 h after removal of the drug, with more normal bacteria present 48 h after removal. For A22, evidence of secondary infection 48 h after antibiotic removal was detected. However, for Rif and Bic, we observed very few, if any, mature inclusions after antibiotic removal from the medium. Thus, Bic more closely resembles the known cidal antibiotic Rif than the static antibiotics Pen and A22. We conclude from these data that Bic is likely a cidal antibiotic to Chlamydia, depending on dosage, with the caveat that the stability of the drug in culture may not allow for an accurate assessment of its activity.

Transcript abundance at the 3' end of the Trp codon-rich ytg operon is increased after bicyclomycin treatment in IFN-y-mediated persistent C. pneumoniae. We previously demonstrated that operons and large genes that are rich in Trp codons at their 5' end had significantly lower levels of transcripts at their 3' end during IFN-γ-mediated Trp starvation in C. pneumoniae. To test whether Rho-mediated polarity was leading to the decrease in abundance of the 3' transcripts, we collected nucleic acid samples from IFN-γ-treated, C. pneumoniae-infected cultures at two different time points after the addition of Bic. We performed short treatments to avoid any potential cidal effect of Bic on the chlamydiae. If Rho were functioning to stop transcription after Trp-rich sequences, then the abundance of the transcript 3' to these sequences should increase after blocking Rho activity. We used the Trp codon-rich ytg and Trp codonpoor rnhB 1 operons (with the Trp codon-rich metG at the 3' end [29]), as well as the Trp codon-rich large gene greA and the Trp codon-free bicistronic operon clpP2X, to test this, as we have extensively assessed their transcription during Trp starvation (28, 29). As previously observed for the ytq operon, the 5' gene, ytqA, was significantly elevated in transcription and much more abundant (\sim 50×) than the 3' gene, ytqD, which is downstream of the Trp codon-rich ytqC gene (Fig. 7A) ([29]). For greA, the 5' end (measured after three Trp codons) was approximately 2-fold more abundant than its 3' end (measured after eight Trp codons) (Fig. 7B). Conversely, for the rnhB_1 operon, the 5' gene, rnhB_1, was less than 2-fold more abundant than the 3' gene, metG, when using a primer set targeting the 5' end of the Trp codon-rich metG gene (Fig. 7C) (29). However, the 3' end of metG was 2-fold less abundant than its 5' end when using a primer set downstream of 5 of 8 Trp codons (29). The clpP2 transcripts were less than 2-fold more abundant than *clpX* transcripts (Fig. 7D).

Interestingly, we observed that, after 2 h of Bic treatment, the abundance of ytgD was approximately 3-fold less than that of ytgA, a change of roughly 20-fold. Similarly, for greA, both its 5' and 3' ends were not statistically distinguishable after Bic addition. Collectively, these data indicate that inhibition of Rho leads to a significant increase in the abundance of transcripts downstream of Trp codon-rich sequences. This is consistent with the hypothesis that Rho-dependent polarity is mediating transcript instability

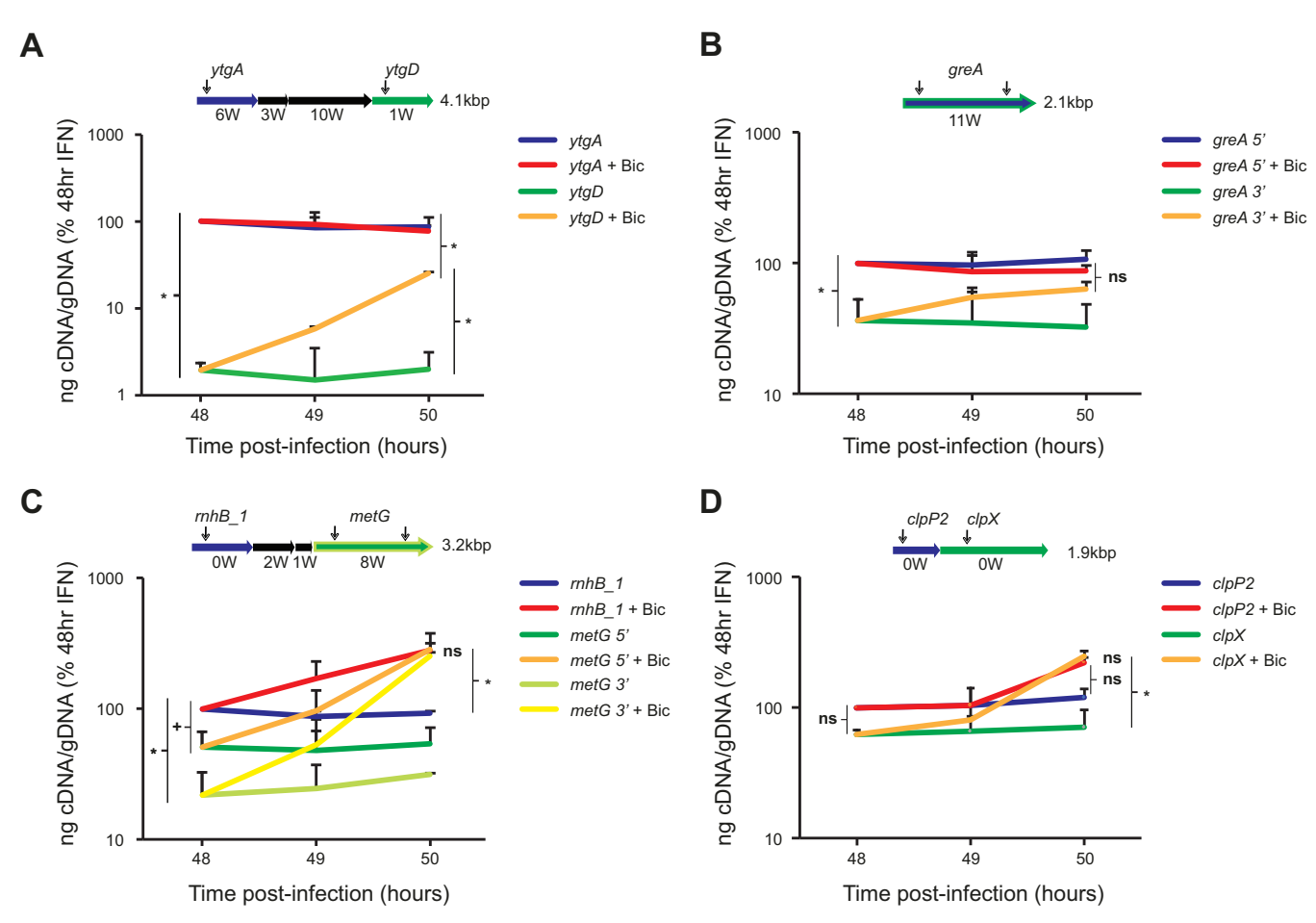


FIG 7 Transcript abundance at the 3' end of messages is increased after bicyclomycin treatment in IFN- γ -mediated persistent *Chlamydia pneumoniae*. HEp2 cells were infected with *C. pneumoniae* AR39 and treated with interferon gamma at the time of infection. At 48 hpi, bicyclomycin (Bic) was added to a subset of wells. Nucleic acid samples were collected at this time point and at 49 and 50 hpi (1 and 2 h posttreatment). Transcript levels were quantified by RT-qPCR and normalized to genomic DNA levels, expressed as nanograms of cDNA/gDNA on the *y* axis. Normalized transcript levels were expressed as a percentage of the 48-h IFN data point. Transcript levels of *ytgA* and *ytgD* (A), of *greA* measured at both its 5' and 3' ends (B), of *rnhB_1* and *metG*, with the latter measured at both its 5' and 3' ends (C), and of *clpP2* and *clpX* (D). Above each graph is a schematic representation of the operon or gene with the indicated numbers of tryptophan (W) codons and the relative position of the qPCR primer sets used (downward arrows). Also shown is the approximate size of the transcript. Data are the averages from at least three experiments analyzed in triplicate. Significance levels as measured by two-tailed, unpaired Student's *t* test between the 5' and 3' ends during IFN treatment with or without Bic: *, P < 0.005; +, P < 0.025; ns, not significant.

downstream of Trp codon-rich sequences during Trp starvation. For the Trp codon-poor $rnhB_1$ operon, the levels of $rnhB_1$ and metG (at both its 5' and 3' ends) were nearly identical, as was true for clpP2X. Furthermore, $rnhB_1$ and clpX transcript levels increased modestly after Bic addition compared to IFN treatment alone. This suggests that there may be internal rut sites within these operons as well and that Rho termination may occur at some frequency in these transcripts. Alternatively, Rho may play a role at the level of the promoter. Both of these possibilities are under investigation.

Transcript abundance at the 3' end of the Trp-codon rich ytg operon is increased after bicyclomycin treatment in IFN- γ -mediated persistent *C. trachomatis* serovar L2. To determine whether the effect of bicyclomycin on transcript abundance during IFN- γ -mediated tryptophan starvation was unique to *C. pneumoniae* or common in *Chlamydia* during persistence, we initiated studies to test the effects of bicyclomycin in persistent *C. trachomatis* serovar L2. This serovar of *C. trachomatis* is rapidly growing and less sensitive to amino acid limitation than *C. pneumoniae* (24), and there are no studies demonstrating bona fide persistence for *C. trachomatis* L2. Consequently, our initial attempts to induce persistence of *C. trachomatis* L2 with IFN- γ failed. We tested pretreatment at various doses and for various times without success.

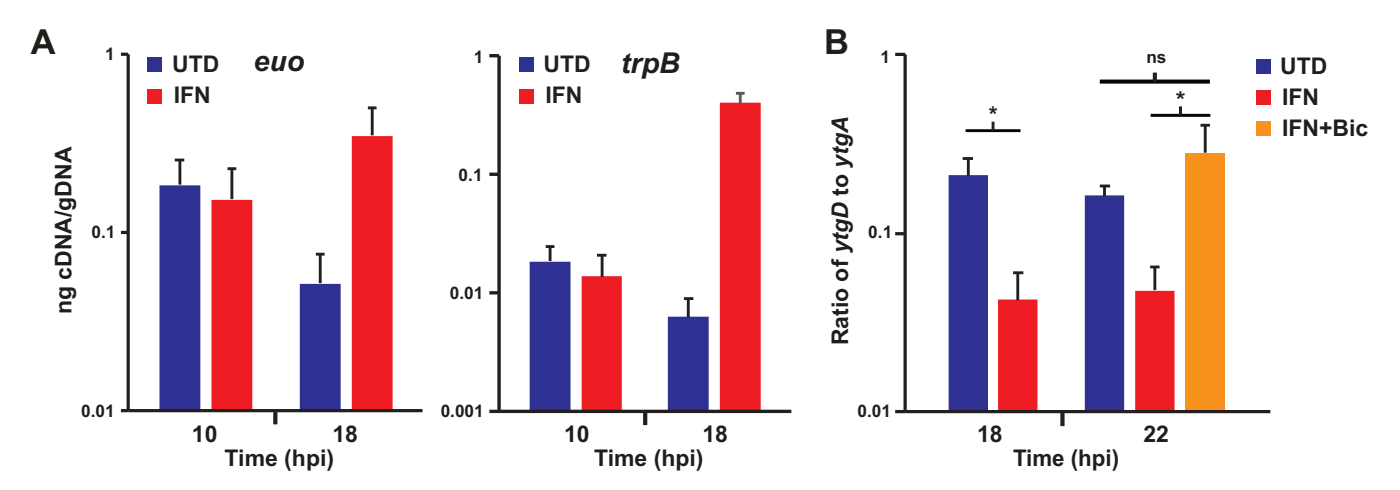


FIG 8 Transcript abundance of ytgD increases in proportion to ytgA after bicyclomycin treatment during IFN-γ-mediated persistence in Chlamydia trachomatis serovar L2. HEp2 cells were pretreated or not (untreated; UTD) with interferon gamma 11 h prior to infection with C. trachomatis serovar L2. Medium was replaced with interferon gamma-conditioned medium at 10 hpi in those samples pretreated with interferon gamma. (A) Measurement of persistence-associated transcripts for euo and trpB at 10 and 18 hpi. Transcript levels were quantified by RT-qPCR, normalized to genomic DNA levels, and expressed as nanograms of cDNA/gDNA on the y axis. (B) At 18 hpi, bicyclomycin (Bic) was added to a subset of interferon gamma-treated wells. Nucleic acid samples were collected at this time point and at 22 hpi (4 h posttreatment). Transcript levels were quantified by RT-qPCR, normalized to genomic DNA levels, and expressed as the ratio of ytgD to ytgA. Data are the averages from at least three experiments analyzed in triplicate with the exception of euo, which was measured from two experiments. Significance levels as measured by two-tailed, unpaired Student's t test between the IFN treatment with or without Bic compared to UTD: *, P < 0.005; ns, not significant.

We also attempted to add medium lacking tryptophan at various times postinfection, also without success. In each instance, we either failed to induce persistence or completely abrogated chlamydial growth. Therefore, we investigated a combination of approaches. Eleven hours prior to infection, HEp2 cells were treated with a low dose of IFN- γ . At 10 hpi, the medium was replaced with IFN- γ -conditioned medium prepared from uninfected cells. The rationale was that IDO would be induced and active by 10 hpi, but the medium would still have sufficient tryptophan to support C. trachomatis L2 growth, based on our earlier failed attempts, and was thus replaced by medium depleted of tryptophan. This approach resulted in the increase in classical persistence transcripts for C. trachomatis, including euo and trpB (Fig. 8A) (28, 52) as well as aberrant morphological forms (data not shown). We next tested the effect of bicyclomycin on transcript abundance in the ytq operon. As with C. pneumoniae, bicyclomycin led to an increase in abundance of ytgD compared to ytgA in IFN- γ -treated cultures (Fig. 8B). Bicyclomycin treatment had no effect on euo or trpB transcript abundance (data not shown). Therefore, the role of Rho-dependent polarity in mediating transcript termination downstream of Trp codons during Trp-limiting conditions is likely common among Chlamydia.

DISCUSSION

The effects of IFN- γ in activating cells to block chlamydial growth have been well characterized over the course of several decades (53–55). As it pertains to human cells infected with *Chlamydia*, the primary mechanism whereby chlamydial growth is inhibited is by depletion of intracellular tryptophan (Trp) pools via activation of the Trpcatabolizing enzyme, indoleamine-2,3-dioxygenase (IDO) (21, 56). Subsequent studies attempting to characterize the effects of Trp starvation on chlamydiae revealed that the developmental cycle is stalled, with the bacteria blocked in division, resulting in aberrantly enlarged RB forms (14, 22, 27). This was referred to as "persistence." Persistent chlamydiae remain viable such that removal of IFN- γ from the culture medium results in the organisms reentering the developmental cycle with continued RB growth and division and the production of EBs. Although these effects have been characterized *in vitro* in cell culture, the ability of chlamydiae to persist may have potential *in vivo* disease relevance (20), and thus a better understanding of the

mechanisms governing chlamydial persistence may result in better diagnostic and therapeutic strategies.

Chlamydial persistence is not equivalent to persistence as characterized in other bacteria, even if the phenotypic effects are similar in terms of reduced growth and resistance to stressful stimuli. In evolving to obligate intracellular dependence, chlamydiae have streamlined their genomic content and eliminated genes primarily associated with nutrient anabolic pathways (3). In contrast to other bacterial species in which persisters are induced by the combined effects of the stringent response (i.e., ppGpp) and toxin-antitoxin systems (57), Chlamydia lacks such responses (3). Thus, how Chlamydia becomes persistent is an interesting microbiological question. Initial attempts at characterizing the molecular mechanisms controlling chlamydial persistence have focused on transcriptional changes in response to Trp limitation via IDO induction. However, chlamydial transcription becomes disconnected from translation during IFN- γ -mediated Trp starvation, with transcription globally increased while translation is globally decreased (28). Thus, there was no convincing evidence for a regulon controlling persistence in response to amino acid limitation. Rather, we recently demonstrated that chlamydial transcription during Trp limitation is dependent on the Trp codon content of the gene being transcribed (29). We found that Trp codon-rich transcripts were preferentially elevated during Trp starvation whereas Trp codon-poor transcripts were unaffected. This unusual finding carried a surprising caveat: transcript abundance, regardless of Trp codon content, was significantly decreased downstream of Trp codon-rich sequences. This resulted in an apparent contradiction of our findings in two main scenarios: operons and large genes. In these cases, Trp codon-rich sequences downstream of a Trp codon-rich 5' region of an operon or gene appeared inconsistent with our model. Similarly, Trp codon-rich sequences downstream of a Trp codon-poor 5' region of an operon or gene followed the Trp codon-poor pattern of transcription. In spite of these exceptions, the effect of Trp codons on the transcription of chlamydial genes during Trp starvation was still detectable by microarray analyses (29). The goal of the current study was to better understand how transcripts become destabilized downstream of Trp codon-rich sequences.

We initially proposed two hypotheses to explain how ribosome stalling at Trp codons could destabilize downstream transcripts (Fig. 1): (i) RNase degradation of unprotected 3' transcripts and (ii) Rho-dependent polarity. In investigating the first possibility, we found no effect of Trp codon content on the stability of transcripts. However, we did observe that transcripts were generally more stable during IFN- γ mediated Trp starvation. Although this stability increase was observed after 15 min of blocking RNA polymerase activity with rifampin, transcripts do decrease in abundance after extended rifampin treatment (reference 28 and data not shown). This is somewhat surprising and suggests that RNases may be overwhelmed by the generalized increase in transcription that occurs during chlamydial persistence induced by Trp starvation (28). Although the annotated RNases in Chlamydia are generally low in Trp (0 or 1 W codon) and show no change in transcription during IFN- γ -mediated Trp starvation (e.g., rnhB_1 [29]), the putative RNase G gene (encoding 2 W) shows an increase in transcription by microarray consistent with our hypothesis of the effects of Trp codons on transcription (29). Further work will be required to determine the role of RNases during chlamydial persistence.

Seeing no effect of Trp codons in stabilizing transcripts, we investigated the roles of Rho in *Chlamydia* more generally and in transcript instability more specifically. Interestingly, the Rho gene carries no Trp codon, and its transcription is unchanged during IFN- γ -mediated Trp starvation (29). This suggests that the Rho gene will be translated and present during chlamydial persistence. Given the important function of Rho in terminating transcription, we were not surprised by the high level of homology between chlamydial Rho paralogs and distantly related bacterial homologs. However, the presence of an extended N-terminal region apparently unique to chlamydial species is interesting and suggests a potentially conserved, and important, function in *Chlamydiaceae*. We determined that this additional domain was not involved in medi-

ating homotypic interactions of Rho, which functions as a hexamer *in vivo*. Further studies are required to determine the function and importance of this additional domain; however, overexpression of the truncated mutant did have a negative effect on chlamydial inclusion growth and development (data not shown). The prediction that the domain is disordered suggests that an additional cofactor(s) may be needed to facilitate correct folding and/or function of chlamydial Rho. This may in turn act as a mechanism of regulating Rho.

Although we have recently described a means for creating conditional knockouts in Chlamydia based on clustered regularly interspaced short palindromic repeat(s) (CRISPR) interference (58), this technology is not fully developed for population-wide analyses. We therefore took advantage of a well-characterized antibiotic, bicyclomycin (47), that inhibits Rho to investigate its biological function in Chlamydia by a chemical genetic approach. Bicyclomycin effectively blocked chlamydial growth and development, indicating the essential role of Rho in chlamydial biology. We were then able to use bicyclomycin as a tool to address whether Rho was functioning to terminate transcription prematurely in sequences downstream from Trp codons within large genes and operons. Indeed, we observed that this was the case, as bicyclomycin treatment during IFN- γ -mediated Trp starvation resulted in the rapid accumulation of ytqD transcripts, which are ordinarily present at levels \sim 80-fold lower than those of the ytgA transcripts. Similar results were observed for both C. pneumoniae and C. trachomatis. During normal growth and development, ytqA transcripts are approximately 6-fold more abundant than ytqD transcripts (Fig. 8) (29). As it is difficult to design reliable primer sets at the 5' and 3' ends of smaller open reading frames (ORFs), we focused on large genes and operons to test the role of Rho in the premature termination of transcription in Trp codon-rich sequences. Furthermore, to detect an effect of Rho-dependent polarity in a smaller ORF (i.e., a measurable decrease in abundance at the 3' end) might require a density of Trp codons not realized until the end of the ORF. Anecdotally, we did not see an effect of bicyclomycin on either Trp codon-rich or -poor transcript abundance for smaller ORFs during IFN-γ-mediated Trp starvation in C. pneumoniae (our unpublished observation) using the single primer sets previously characterized (29). We conclude from these data that Rho is essential in Chlamydia and likely mediating, at least in part, functions similar to those that it mediates in other bacteria.

Although Rho may perform similar functions in Chlamydia and in E. coli, for example, there still remain several outstanding questions. Typical Rho binding sites, called rut sites (for Rho utilization) (59, 65), are C-rich sequences because these sequences are often unstructured and facilitate Rho translocation along the transcript. Chlamydia species are AT-rich organisms with a GC content of \sim 40% (3). Therefore, one project being pursued in the lab is the identification of chlamydial rut sites as well as genes whose transcripts are terminated extrinsically by Rho instead of by intrinsic termination factors. Rho has been characterized as an important mediator of a variety of bacterial processes beyond its function as a bona fide transcriptional terminator. Recent evidence suggests a role for Rho in blocking antisense transcription and R-loop formation while acting as a transcriptional regulator by recruitment via riboswitches and by small RNA (sRNA)-induced polarity (36). Based on our current data, we cannot exclude a role for riboswitches in mediating premature transcript termination or ribosome stalling during amino acid starvation, but this does not exclude a role for Rho in these processes. While it is also of great interest to determine when Rho terminates transcription during a normal developmental cycle in Chlamydia, we are also exploring what other functions it may have as a global regulator.

ment (28): the approach that we implemented here to induce persistence in serovar L2 may provide a means for this. The fact that Chlamydia has evolved to eliminate the systems normally employed by bacteria to induce persister cells yet retains the ability to persist in eukaryotic cells suggests either that the chlamydial system represents an evolutionary precursor (i.e., devolved) to a persister phenotype or that chlamydiae may have evolved a novel, specific mechanism to arrive at the same endpoint. Regardless of which may be true, a better understanding of chlamydial persistence may yield surprising benefits ranging from synthetic organism design to novel diagnostic and therapeutic strategies. The current work has furthered our understanding of a key observation of chlamydial persistence mediated by amino acid starvation and revealed an important role for Rho in this process. It is likely that Rho will play additional important roles in chlamydial biology.

MATERIALS AND METHODS

Organisms and cell culture. C. pneumoniae AR39 EBs or C. trachomatis serovar L2 EBs were harvested from infected HEp-2 cell cultures at 35°C or 37°C, respectively, with 5% CO2 and density gradient purified, and their titers for infectivity were measured by determining inclusion-forming units (IFU) on fresh cell monolayers. The human epithelial cell line HEp-2 was routinely cultivated at 37°C with 5% CO₂ in Iscove's modified Dulbecco's medium (IMDM) containing Glutamax, glucose, HEPES, and sodium bicarbonate (Gibco/ThermoFisher, Waltham, MA) supplemented with 10% fetal bovine serum (FBS; Sigma, St. Louis, MO). The mouse fibroblast cell line McCoy was used for transforming C. trachomatis L2 and was routinely cultivated in Dulbecco's modified Eagle medium (DMEM; Gibco) supplemented with 10% FBS. The HEp-2 and McCoy cells were a kind gift of H. Caldwell (NIH/NIAID). Recombinant human interferon gamma (IFN- γ) was purchased from Cell Sciences (Canton, MA) and resuspended to 100 μ g ml⁻¹ in 0.1% bovine serum albumin (BSA; Sigma) diluted in water. Aliquots were frozen at -80°C and used only once to avoid freeze-thawing. IFN- γ was titrated for its effect to induce persistence without killing the bacteria and, in our experiments, was used at 2 ng ml⁻¹ and added at the time of infection for C. pneumoniae. For C. trachomatis, 0.5 ng ml^{-1} was added to cells approximately 11 h prior to infection. Medium was replaced at 10 hpi with IFN-y-conditioned medium (ICM) to induce persistence in C. trachomatis. ICM was prepared by adding 2 ng ml⁻¹ IFN-γ to uninfected HEp2 cells for approximately 54 h prior to collection and filtration of the medium. To determine the half-life of C. pneumoniae transcripts in the presence or absence of IFN- γ , 1 μ g ml⁻¹ rifampin (Rif; Sigma) was added directly to the wells at the indicated time points to inhibit RNA polymerase. Nucleic acid samples were collected 15 or 30 min after rifampin addition (see below). To determine the effects of bicyclomycin (Bic) on transcript abundance, 25 μg ml $^{-1}$ Bic (Cayman Chemical, Ann Arbor, MI) was added to C. pneumoniae-infected IFN-γ-treated cultures at 48 hpi and for C. trachomatis-infected IFN-γ-treated cultures at 18 hpi, with samples subsequently collected at the indicated time points.

Nucleic acid extraction and RT-qPCR. For transcript analyses, HEp-2 cells were plated in 6-well plates at a density of 10⁶ per well and infected at a multiplicity of infection (MOI) of 2 with C. pneumoniae AR39 or an MOI of 1 for C. trachomatis L2. In some wells, cells were plated and infected on coverslips to monitor the infection and progression to persistence (see "Immunofluorescence analysis of the effects of antibiotics on chlamydial inclusion formation" below). Assays to quantify the indicated transcripts were performed essentially as described previously (28, 29, 60). Briefly, total RNA was collected from infected cells at the indicated times using TRIzol (Invitrogen/ThermoFisher) and rigorously treated with Turbo DNAfree (Ambion/ThermoFisher) to remove contaminating DNA according to the manufacturer's guidelines. One microgram of DNA-free RNA was reverse transcribed or not with random nonamers (New England BioLabs, Ipswich, MA) using SuperScript III RT (Invitrogen/ThermoFisher) according to the manufacturer's instructions. The RT and no-RT reaction mixtures were diluted 10-fold with water, aliquoted, and stored at -80°C. Equal volumes of each reaction mixture were used in 25-µl qPCR mixtures with SYBR green (Quanta Biosciences, Gaithersburg, MD) and quantified on an ABI 7300 system (Applied Biosystems/ThermoFisher) using the standard amplification cycle with a melting curve analysis. Results were compared to a standard curve generated against purified C. pneumoniae or C. trachomatis L2 genomic DNA as appropriate. Duplicate DNA samples were collected from the same experiment using the DNeasy tissue kit (Qiagen). Chlamydial genomes were quantified from equal amounts of total DNA by qPCR using the euo primer set and used to normalize transcript data as described previously (28, 29, 60). RT-qPCR results were corrected for efficiency (typically above 90% with r^2 values above 0.999). The half-life $(t_{1/2})$ of transcripts was calculated using the formula $t_{1/2} = t/\{\log_2(N_0) - \log_2[N(t)]\}$, where trepresents the 15 min of treatment with Rif, No is the amount of transcript measured at the time of addition of Rif, and N(t) is the amount of transcript measured after 15 min of Rif treatment. Primer sequences are listed in Table S1 in the supplemental material and were designed using the PrimerQuest Tool (Integrated DNA Technologies, Coralville, IA) based on the C. pneumoniae CWL029 sequence available from the STD sequence database (http://stdgen.northwestern.edu) or C. trachomatis serovar L2 sequence available from NCBI (https://www.ncbi.nlm.nih.gov/gene/). Results were graphed using Microsoft Excel. Student's two-tailed t test was used for the determination of significance of differences between the untreated and IFN- γ -treated samples.

Bioinformatics analyses. Sequences and gene maps for C. trachomatis serovar D were obtained from the STD sequence database (http://stdgen.northwestern.edu), for E. coli from the Ecogene 3.0

project (http://ecogene.org), and for M. tuberculosis from the NCBI Gene database (https://www.ncbi.nlm .nih.gov/gene/). Other chlamydial Rho sequences were searched via NCBI. Alignments were performed using the NCBI Protein BLAST function (Fig. 3C) (61). The protein disorder probabilities were calculated using the protein disorder prediction system (http://prdos.hgc.jp) with a false-positive prediction rate of 5% (66).

Plasmid construction. A complete list of primers and plasmids is available in Table S1 in the supplemental material. For bacterial two-hybrid studies, the plasmids pKT25 and pUT18C were digested with Xbal and Kpnl and treated with alkaline phosphatase (all enzymes from Fermentas/ThermoFisher). PCR products of full-length rho or a truncation of rho lacking the first 49 amino acids, Rho50, were generated from C. trachomatis L2 with flanking Xbal and Kpnl sites and subsequently digested with these enzymes. The digested plasmids and PCR products were ligated using T4 ligase (Fermentas) and transformed into chemically competent E. coli XL1 (Stratagene/Agilent, Santa Clara, CA) and plated on Luria agar containing 0.4% glucose and appropriate antibiotics. Positive clones were sequence verified by Eurofins Genomics (Louisville, KY). For chlamydial transformation plasmids encoding Rho-6×His or Rho50-6×His, a first PCR product was generated to add the 6×His tag to chlamydial rho. A second PCR product was generated using the first product as the template to add flanking regions for Gibson-type cloning into the anhydrotetracycline (aTc)-inducible plasmid pASK linearized with Agel (42). To mutate the Walker B motif (D311A) of Rho (RhoBmut), the Q5 mutagenesis kit (New England BioLabs) was used according to the manufacturer's instructions using the primers listed in Table S1 and the pKT25-rho vector as the template. A PCR product encoding a 6×His tag at the 3' end was then generated (using the mutated pKT25-rho vector as the template for the first reaction) as described above for cloning into pASK. The plasmid encoding the rho product was assembled using the NEBuilder HiFi DNA assembly kit (New England BioLabs) according to the manufacturer's instructions. PCR primers for the assembly were designed using the NEBuilder assembly tool (http://nebuilder.neb.com/). The pASK-rho plasmids were sequence verified and used to transform an E. coli strain with deletion of genes dam and dcm, E. coli Δdam Δdcm (New England BioLabs), from which demethylated plasmid midipreps (Qiagen) were prepared, sequence verified, and used to transform C. trachomatis serovar L2 (see below).

Bacterial protein-protein interactions. Bacterial adenylate cyclase two-hybrid (BACTH) interactions were performed as described elsewhere (43, 62) using the adenylate cyclase mutant (Δcya) strain DHT1 of E. coli. Briefly, chemically competent DHT1 cells were cotransformed with plasmids encoding the chlamydial Rho proteins (truncated or full length) fused to the C terminus of the T25 or T18 fragment of adenylate cyclase from Bordetella pertussis. Separately, positive (L-zip-encoding) and negative (empty vector) control plasmids were also cotransformed into DHT1 cells. Transformed bacteria were plated on M63 minimal medium agar containing selective antibiotics, 40 μg ml $^{-1}$ X-Gal (5-bromo-4-chloro-3 $indolyl-\beta-\text{D-galactopyranoside}),~0.5~\text{mM IPTG (isopropyl-}\beta-\text{D-thiogalactopyranoside)},~\text{and}~0.2\%~\text{maltose}$ (39, 50). Plates were incubated at 30°C for up to 5 days to detect interactions between the Rho constructs. Robust growth with blue colonies on minimal medium plates occurs only when adenylate cyclase activity is reconstituted by interacting proteins to activate the mal and lac operons (63, 64).

Chlamydial transformation. C. trachomatis serovar L2 lacking the endogenous plasmid (-pL2) was transformed according to the protocol of Mueller and Fields (45) using the aTc-inducible plasmids encoding either Rho_6×His, Rho50_6×His, or RhoBmut_6×His. Briefly, 2 µg of demethylated plasmid was used to transform 106 EBs in Tris-CaCl₂ buffer (41) for 30 min at room temperature. This transformation inoculum was used to infect a confluent layer of McCoy cells by centrifugation at 400 imes g for 15 min followed by incubation at 37°C for 15 min. The inoculum was aspirated, and DMEM only was added to the well. After 8 h of infection, the medium was replaced with DMEM containing 1 U ml⁻¹ penicillin. Infected cells were passaged at 48 h postinfection and every 48 h thereafter until penicillin-resistant bacteria were isolated.

Determination of the effect of overexpression of Rho-6×His transformants in C. trachomatis L2 by immunofluorescence analysis. For C. trachomatis L2 transformed strains expressing anhydrotetracyline (aTc)-inducible, C-terminal 6×His-tagged Rho variants, HEp2 cells plated on coverslips were infected and treated with penicillin as a selecting agent, and 10 nM aTc was added or not at 10 hpi. Cells were subsequently fixed in methanol at 16 or 24 hpi and stained with primary mouse antibody against the 6×His tag (GenScript, Piscataway, NJ) and secondary Alexa 594-conjugated goat anti-mouse antibody (Thermo Fisher) to detect Rho-6×His. To detect the chlamydial organisms directly, a primary guinea pig antichlamydial antibody (kind gift of Elizabeth Rucks, University of Nebraska Medical Center [UNMC]) was used, followed by a secondary Alexa 488-conjugated goat anti-guinea pig antibody. Cell nuclei and bacterial DNA were visualized with DAPI (4',6-diamidino-2-phenylindole). Images were acquired on an LSM710 Zeiss confocal microscope, with a $40 \times$ objective and $4 \times$ digital zoom, located within the UNMC Advanced Microscopy Core. Images were minimally processed for brightness/contrast using Adobe Photoshop Creative Cloud 2017.

Quantification of inclusion-forming units after bicyclomycin treatment. To determine the effect of bicyclomycin (Bic), an antibiotic that targets Rho, on chlamydial growth, HEp-2 cells were plated in 24-well plates. Cells were infected with C. trachomatis L2 at an MOI of 1 and treated at the indicated time point with the indicated concentration of Bic. At 24 hpi, infected cells were scraped in sucrose storage medium (2SP [41]) and collected into 1.5-ml microcentrifuge tubes containing 3 glass beads. Samples were vortexed for 1 min and frozen at -80° C. The frozen samples were thawed, serially 10-fold diluted, and used to infect a fresh cell layer of HEp-2 seeded in 24-well plates. After 24 hpi, the infected cells were fixed and stained with a primary guinea pig antichlamydial antibody (kind gift of Elizabeth Rucks, UNMC) followed by a secondary Alexa 488-conjugated goat anti-guinea pig antibody. Fluorescent inclusions were counted from 15 fields of view at a magnification of \times 20, the average of which was multiplied by

the fields of view per well and the inverse of the dilution counted. Taking into account the volume of inoculum used from the serial dilution, the calculation is reported as IFUs recovered.

Immunofluorescence analysis of the effects of antibiotics on chlamydial inclusion formation. HEp2 cells were plated in 24-well plates on coverslips and infected the following day with *C. trachomatis* serovar L2 at an MOI of 0.5. At 8 hpi, the indicated antibiotics were added to the medium. Penicillin (Pen) was used at 1 U/ml, A22 was used at 75 μ M, rifampin (Rif) was used at 1 μ g ml⁻¹, and bicyclomycin (Bic) was used at 25 μ g ml⁻¹. At 24 hpi, a subset of coverslips was fixed in methanol at room temperature for 5 min. The remaining coverslips were rinsed three times with Hanks' balanced salt solution, and fresh medium without antibiotics was added to the wells to allow for reactivation of chlamydial growth. At 48 hpi (24-h reactivation) and 72 hpi (48-h reactivation), a subset of wells was fixed in methanol. All coverslips were stained with a primary guinea pig antichlamydial antibody (kind gift of Elizabeth Rucks, UNMC) followed by a secondary Alexa 488-conjugated goat anti-guinea pig antibody to visualize inclusions. Images were acquired on an LSM710 Zeiss confocal microscope, with a 20× objective to capture a wide field of view, located within the UNMC Advanced Microscopy Core. Images were minimally processed for brightness/contrast using Adobe Photoshop Creative Cloud 2017.

SUPPLEMENTAL MATERIAL

Supplemental material for this article may be found at https://doi.org/10.1128/IAI .00240-18.

SUPPLEMENTAL FILE 1, PDF file, 0.2 MB.

ACKNOWLEDGMENTS

We thank Kelsey Rueden and Janice A. Taylor for technical assistance, H. Caldwell (NIAID/NIH) for eukaryotic cell stocks, and E. Rucks for the antibody against *Chlamydia* and for critical review of the manuscript.

Support for the UNMC Advanced Microscopy Core Facility was provided by the Nebraska Research Initiative, the Fred and Pamela Buffett Cancer Center Support Grant (P30CA036727), and an Institutional Development Award (IDeA) from the NIGMS/NIH (P30GM106397). The NIH SIG-funded LSM710 Zeiss confocal microscope was supported by NIH S10RR027301. S.P.O. was supported by start-up funds from the University of South Dakota and University of Nebraska Medical Center as well as a CAREER award (number 1810599) from the National Science Foundation.

We declare that we have no conflict of interest.

REFERENCES

- Abdelrahman YM, Belland RJ. 2005. The chlamydial developmental cycle. FEMS Microbiol Rev 29:949–959. https://doi.org/10.1016/j.femsre.2005 03.002
- Moore ER, Ouellette SP. 2014. Reconceptualizing the chlamydial inclusion as a pathogen-specific parasitic organelle: an expanded role for Inc proteins. Front Cell Infect Microbiol 4:157. https://doi.org/10.3389/fcimb 2014 00157.
- Stephens RS, Kalman S, Lammel C, Fan J, Marathe R, Aravind L, Mitchell W, Olinger L, Tatusov RL, Zhao Q, Koonin EV, Davis RW. 1998. Genome sequence of an obligate intracellular pathogen of humans: *Chlamydia trachomatis*. Science 282:754–759. https://doi.org/10.1126/science.282 .5389.754.
- Schachter J, Storz J, Tarizzo ML, Bogel K. 1973. Chlamydiae as agents of human and animal diseases. Bull World Health Organ 49:443–449.
- Grayston JT. 1992. Infections caused by Chlamydia pneumoniae strain TWAR. Clin Infect Dis 15:757–761. https://doi.org/10.1093/clind/15.5.757.
- Mabey DCW, Solomon AW, Foster A. 2003. Trachoma. Lancet 362: 223–229. https://doi.org/10.1016/S0140-6736(03)13914-1.
- Datta SD, Sternberg M, Johnson RE, Berman S, Papp JR, McQuillan G, Weinstock H. 2007. Gonorrhea and chlamydia in the United States among persons 14 to 39 years of age, 1999 to 2002. Ann Intern Med 147:89–96. https://doi.org/10.7326/0003-4819-147-2-200707170-00007.
- Brunham RC, MacLean IW, Binns B, Peeling RW. 1985. Chlamydia trachomatis: its role in tubal infertility. J Infect Dis 152:1275–1282. https://doi.org/10.1093/infdis/152.6.1275.
- Taylor-Robinson D, Gilroy CB, Thomas BJ, Keat AC. 1992. Detection of Chlamydia trachomatis DNA in joints of reactive arthritis patients by polymerase chain reaction. Lancet 340:81–82. https://doi.org/10.1016/ 0140-6736(92)90399-N.

- Saikku P, Leinonen M, Mattila K, Ekman WR, Nieminen MS, Mäkelä PH, Huttunen JK, Valtonen V. 1988. Serological evidence of an association of a novel *Chlamydia*, TWAR, with chronic coronary heart disease and acute myocardial infarction. Lancet ii:983–986.
- 11. Hahn DL. 1995. Treatment of *Chlamydia pneumoniae* infection in adult asthma: a before-after trial. J Fam Pract 41:345–351.
- Beatty WL, Morrison RP, Byrne GI. 1994. Persistent chlamydiae: from cell culture to a paradigm for chlamydial pathogenesis. Microbiol Rev 58: 686–699.
- 13. Wyrick PB. 2010. Chlamydia trachomatis persistence in vitro: an overview. J Infect Dis 201:S88–S95. https://doi.org/10.1086/652394.
- Beatty WL, Byrne GI, Morrison RP. 1993. Morphologic and antigenic characterization of interferon gamma-mediated persistent *Chlamydia* trachomatis infection in vitro. Proc Natl Acad Sci U S A 90:3998–4002.
- Raulston JE. 1997. Response of Chlamydia trachomatis serovar E to iron restriction in vitro and evidence for iron-regulated chlamydial proteins. Infect Immun 65:4539 – 4547.
- Thompson CC, Carabeo RA. 2011. An optimal method of iron starvation of the obligate intracellular pathogen, *Chlamydia trachomatis*. Front Microbiol 2:20. https://doi.org/10.3389/fmicb.2011.00020.
- 17. Hatch TP. 1975. Competition between *Chlamydia psittaci* and L cells for host isoleucine pools: a limiting factor in chlamydial multiplication. Infect Immun 12:211–220.
- Harper A, Pogson Cl, Jones ML, Pearce JH. 2000. Chlamydial development is adversely affected by minor changes in amino acid supply, blood plasma amino acid levels, and glucose deprivation. Infect Immun 68:1457–1464. https://doi.org/10.1128/IAI.68.3.1457-1464.2000.
- Jones ML, Gaston JS, Pearce JH. 2001. Induction of abnormal Chlamydia trachomatis by exposure to interferon-gamma or amino acid deprivation

and comparative antigenic studies. Microb Pathog 30:299–309. https://doi.org/10.1006/mpat.2001.0433.

- Lewis ME, Belland RJ, AbdelRahman YM, Beatty WL, Aiyar AA, Zea AH, Greene SJ, Marrero L, Buckner LR, Tate DJ, McGowin CL, Kozlowski PA, O'Brien M, Lillis RA, Martin DH, Quayle AJ. 2014. Morphologic and molecular evaluation of *Chlamydia trachomatis* growth in human endocervix reveals distinct growth patterns. Front Cell Infect Microbiol 4:71. https://doi.org/10.3389/fcimb.2014.00071.
- Byrne GI, Lehmann LK, Landry GJ. 1986. Induction of tryptophan catabolism is the mechanism for gamma-interferon-mediated inhibition of intracellular *Chlamydia psittaci* replication in T24 cells. Infect Immun 53:347–351.
- Beatty WL, Morrison RP, Byrne Gl. 1994. Immunoelectron-microscopic quantitation of differential levels of chlamydial proteins in a cell culture model of persistent *Chlamydia trachomatis* infection. Infect Immun 62: 4059–4062.
- 23. Pfefferkorn ER. 1984. Interferon gamma blocks the growth of *Toxoplasma gondii* in human fibroblasts by inducing the host cells to degrade tryptophan. Proc Natl Acad Sci U S A 81:908–912.
- Ouellette SP, Dorsey FC, Moshiach S, Cleveland JL, Carabeo RA. 2011. Chlamydia species-dependent differences in the growth requirement for lysosomes. PLoS One 6:e16783. https://doi.org/10.1371/journal.pone .0016783.
- Caldwell HD, Wood H, Crane D, Bailey R, Jones RB, Mabey D, MacLean I, Mohammed Z, Peeling R, Roshick C, Schachter J, Solomon AW, Stamm WE, Suchland RJ, Taylor L, West SK, Quinn TC, Belland RJ, McClarty G. 2003. Polymorphisms in *Chlamydia trachomatis* tryptophan synthase genes differentiate between genital and ocular isolate. J Clin Invest 111:1757–1769. https://doi.org/10.1172/JCI17993.
- Aiyar A, Quayle AJ, Buckner LR, Sherchand SP, Chang TL, Zea AH, Martin DH, Belland RJ. 2014. Influence of the tryptophan-indole-IFN axis on human genital *Chlamydia trachomatis* infection: role of vaginal coinfections. Front Cell Infect Microbiol 4:72. https://doi.org/10.3389/fcimb .2014.00072.
- Beatty WL, Morrison RP, Byrne Gl. 1995. Reactivation of persistent Chlamydia trachomatis infection in cell culture. Infect Immun 63:199–205.
- Ouellette SP, Hatch TP, AbdelRahman YM, Rose LA, Belland RJ, Byrne GI. 2006. Global transcriptional upregulation in the absence of increased translation in *Chlamydia* during IFNgamma-mediated host cell tryptophan starvation. Mol Microbiol 62:1387–1401. https://doi.org/10.1111/j .1365-2958.2006.05465.x.
- Ouellette SP, Rueden KJ, Rucks EA. 2016. Tryptophan codon-dependent transcription in *Chlamydia pneumoniae* during gamma interferonmediated tryptophan limitation. Infect Immun 84:2703–2713. https://doi .org/10.1128/IAI.00377-16.
- Peters JM, Vangeloff AD, Landick R. 2011. Bacterial transcription terminators: the RNA 3'-end chronicles. J Mol Biol 412:793–813. https://doi.org/10.1016/j.jmb.2011.03.036.
- 31. Ferreira R, Borges V, Borrego MJ, Gomes JP. 2017. Global survey of mRNA levels and decay rates of *Chlamydia trachomatis* trachoma and lymphogranuloma venereum biovars. Heliyon 3:e00364. https://doi.org/10.1016/j.heliyon.2017.e00364.
- Laalami S, Zig L, Putzer H. 2014. Initiation of mRNA decay in bacteria. Cell Mol Life Sci 71:1799–1828. https://doi.org/10.1007/s00018-013-1472-4.
- 33. Richardson JP, Grimley C, Lowery C. 1975. Transcription termination factor rho activity is altered in *Escherichia coli* with suA gene mutations. Proc Natl Acad Sci U S A 72:1725–1728.
- Richardson JP, Carey JL, III. 1982. Rho factors from polarity suppressor mutants with defects in their RNA interactions. J Biol Chem 257: 5767–5771.
- 35. Wek RC, Sameshima JH, Hatfield GW. 1987. Rho-dependent transcriptional polarity in *ilvGMEDA* operon of wild-type *Escherichia coli* K12. J Biol Chem 262:15256–15261.
- Boudvillain M, Figueroa-Bossi N, Bossi L. 2013. Terminator still moving forward: expanding roles for Rho factor. Curr Opin Microbiol 16: 118–124. https://doi.org/10.1016/j.mib.2012.12.003.
- Mitra P, Ghosh G, Hafeezunnisa M, Sen R. 2017. Rho protein: roles and mechanisms. Annu Rev Microbiol 71:687–709. https://doi.org/10.1146/ annurev-micro-030117-020432.
- 38. Yuan AH, Hochschild A. 2017. A bacterial global regulator forms a prion. Science 355:198–201. https://doi.org/10.1126/science.aai7776.
- Karimova G, Pidoux J, Ullmann A, Ladant D. 1998. A bacterial two-hybrid system based on a reconstituted signal transduction pathway. Proc Natl Acad Sci U S A 95:5752–5756.

 Belland RJ, Zhong G, Crane DD, Hogan D, Sturdevant D, Sharma J, Beatty WL, Caldwell HD. 2003. Genomic transcriptional profiling of the developmental cycle of *Chlamydia trachomatis*. Proc Natl Acad Sci U S A 100:8478–8483. https://doi.org/10.1073/pnas.1331135100.

- Wang Y, Kahane S, Cutcliffe LT, Skilton RJ, Lambden PR, Clarke IN. 2011. Development of a transformation system for *Chlamydia trachomatis*: restoration of glycogen biosynthesis by acquisition of a plasmid shuttle vector. PLoS Pathog 7:e1002258. https://doi.org/10.1371/journal.ppat.1002258.
- 42. Wickstrum J, Sammons LR, Restivo KN, Hefty PS. 2013. Conditional gene expression in *Chlamydia trachomatis* using the Tet system. PLoS One 8:e76743. https://doi.org/10.1371/journal.pone.0076743.
- Ouellette SP, Rueden KJ, AbdelRahman YM, Cox JV, Belland RJ. 2015. Identification and partial characterization of potential FtsL and FtsQ homologs in *Chlamydia*. Front Microbiol 6:1264. https://doi.org/10.3389/ fmicb.2015.01264.
- Rucks EA, Olson MG, Jorgenson LM, Srinivasan RR, Ouellette SP. 2017.
 Development of a proximity labeling system to map the *Chlamydia trachomatis* inclusion membrane. Front Cell Infect Microbiol 7:40. https://doi.org/10.3389/fcimb.2017.00040.
- 45. Mueller KE, Fields KA. 2015. Application of β-lactamase reporter fusions as an indicator of effector protein secretion during infections with the obligate intracellular pathogen *Chlamydia trachomatis*. PLoS One 10: e0135295. https://doi.org/10.1371/journal.pone.0135295.
- Johnson CM, Fisher DJ. 2013. Site-specific, insertional inactivation of *incA* in *Chlamydia trachomatis* using a group II intron. PLoS One 8:e83989. https://doi.org/10.1371/journal.pone.0083989.
- 47. Zwiefka A, Kohn H, Widger WR. 1993. Transcription termination factor rho: the site of bicyclomycin inhibition in *Escherichia coli*. Biochemistry 32:3564–3570. https://doi.org/10.1021/bi00065a007.
- Park HG, Zhang X, Moon HS, Zwiefka A, Cox K, Gaskell SJ, Widger WR, Kohn H. 1995. Bicyclomycin and dihydrobicyclomycin inhibition kinetics of *Escherichia coli* rho-dependent transcription termination factor ATPase activity. Arch Biochem Biophys 323:447–454. https://doi.org/10 .1006/abbi.1995.0066.
- 49. Miyairi I, Mahdi OS, Ouellette SP, Belland RJ, Byrne GI. 2006. Different growth rates of *Chlamydia trachomatis* biovars reflect pathotype. J Infect Dis 194:350–357. https://doi.org/10.1086/505432.
- 50. Ouellette SP, Karimova G, Subtil A, Ladant D. 2012. *Chlamydia* co-opts the rod shape-determining proteins MreB and Pbp2 for cell division. Mol Microbiol 85:164–178. https://doi.org/10.1111/j.1365-2958.2012 .08100.x.
- 51. Bowie WR, Lee CK, Alexander ER. 1978. Prediction of efficacy of antimicrobial agents in treatment of infections due to *Chlamydia trachomatis*. J Infect Dis 138:655–659. https://doi.org/10.1093/infdis/138.5.655
- Wood H, Fehlner-Garnder C, Berry J, Fischer E, Graham B, Hackstadt T, Roshick C, McClarty G. 2003. Regulation of tryptophan synthase gene expression in *Chlamydia trachomatis*. Mol Microbiol 49:1347–1359. https://doi.org/10.1046/j.1365-2958.2003.03638.x.
- Rothermel CD, Rubin BY, Murray HW. 1983. Gamma-interferon is the factor in lymphokine that activates human macrophages to inhibit intracellular *Chlamydia psittaci* replication. J Immunol 131:2542–2544.
- Byrne GI, Krueger DA. 1983. Lymphokine-mediated inhibition of *Chlamydia* replication in mouse fibroblasts is neutralized by anti-gamma interferon immunoglobulin. Infect Immun 42:1152–1158.
- 55. Shemer Y, Sarov I. 1985. Inhibition of growth of *Chlamydia trachomatis* by human gamma interferon. Infect Immun 48:592–596.
- Thomas SM, Garrity LF, Brandt CR, Schobert CS, Feng GS, Taylor MW, Carlin JM, Byrne GI. 1993. IFN-gamma-mediated antimicrobial response. Indoleamine 2,3-dioxygenase-deficient mutant host cells no longer inhibit intracellular *Chlamydia* spp. or *Toxoplasma* growth. J Immunol 150:5529–5534.
- Maisonneuve E, Castro-Camargo M, Gerdes K. 2013. (p)ppGpp controls bacterial persistence by stochastic induction of toxin-antitoxin activity. Cell 154:1140–1150. https://doi.org/10.1016/j.cell.2013.07.048.
- Ouellette SP. 2018. Feasibility of a conditional knockout system for Chlamydia based on CRISPR interference. Front Cell Infect Microbiol 8:59. https://doi.org/10.3389/fcimb.2018.00059.
- 59. Chen CY, Galluppi GR, Richardson JP. 1986. Transcription termination at lambda tR1 is mediated by interaction of rho with specific single-stranded domains near the 3' end of cro mRNA. Cell 46:1023–1028. https://doi.org/10.1016/0092-8674(86)90701-4.
- Ouellette SP, AbdelRahman YM, Belland RJ, Byrne Gl. 2005. The Chlamydia pneumonia type III secretion-related IcrH gene clusters are devel-

- opmentally expressed operons. J Bacteriol 187:7853-7856. https://doi .org/10.1128/JB.187.22.7853-7856.2005.
- 61. Altschul SF, Gish W, Miller W, Myers EW, Lipman DJ. 1990. Basic local alignment search tool. J Mol Biol 215:403-410. https://doi.org/10.1016/ 50022-2836(05)80360-2.
- 62. Karimova G, Dautin N, Ladant D. 2005. Interaction network among Escherichia coli membrane proteins involved in cell division as revealed by bacterial two-hybrid analysis. J Bacteriol 187:2233-2243. https://doi .org/10.1128/JB.187.7.2233-2243.2005.
- 63. Ouellette SP, Karimova G, Davi M, Ladant D. 2017. Analysis of membrane protein interactions with a bacterial adenylate cyclase-based two-hybrid
- (BACTH) technique. Curr Protoc Mol Biol 118:20.12.1-20.12.24. https:// doi.org/10.1002/cpmb.36.
- 64. Karimova G, Gauliard E, Davi M, Ouellette SP, Ladant D. 2017. Proteinprotein interaction: bacterial two-hybrid. Methods Mol Biol 1615: 159-176. https://doi.org/10.1007/978-1-4939-7033-9_13.
- 65. Chen CY, Richardson JP. 1987. Sequence elements essential for rhodependent transcription termination at lambda tR1. J Biol Chem 262: 11292-11299.
- 66. Ishida T, Kinoshita K. 2007. PrDOS: prediction of disordered protein regions from amino acid sequence. Nucleic Acids Res 35:W460-W464. https://doi.org/10.1093/nar/gkm363.